Keck 1 HIRES Observations of Tempel 1 at the Time of Impact

W. M. Jackson[1] and A. Cochran[2]

[1] Chemistry Department, University of California, Davis wmjackson@ucdavis.edu
[2] McDonald Observatory, University of Texas anita@barolo.as.utexas.edu

Abstract The Keck 1 HIRES observations of the Deep Impact event on July 4 have been qualitatively re-examined in an effort to isolate the changes in the HIRES spectra that can be attributed to the event itself. To accomplish this goal, background spectra due to ambient emission that was already present in the comet were extracted from the pixels at the end of the slit. This material can not have any emission from material that was produced at the time of the impact until at least several thousand seconds after the impact because it takes this long for the material to reach this distance from the nucleus. With the data extracted in this manner it can be shown that the spectra from OH, O(^{1}S), CN, NH, NH_2, C_2, and C_3 changed as a function of time after impact. In the spectra of all of these species there is evidence for a prompt change in the emission intensity that probably is due to the hot plume formed initially during the impact. After the first 600 s the time dependence of the intensities of the emission spectra species appear to be consistent with the photochemical formation and destruction of parents and daughters. The spectral changes with time associated with the CH emission appear to be unique in that the only change that is observed is right after the impact; at times after this the emission intensity is constant. All of these changes are discussed in terms of the photochemical mechanisms that have been thought to form the observed free radicals in comets.

1 Observations and Reductions

On 4 July 2005 UT, we used the HIRES instrument on the Keck 1 telescope[1] to observe the impact of comet 9P/Tempel 1 with the Deep Impact spacecraft. The impact speed of 10.3 km sec^{-1} resulted in an impact kinetic energy of 19 GJ [2]. The impact occurred at 05:44:36 UT (Earth-received time of 05:52:02 UT).

The HIRES instrument is a cross-dispersed, high spectral resolution spectrograph. We used the blue cross-disperser for our observations, resulting in a

[1] The data presented herein were obtained at the W. M. Keck Observatory, which is operated as a scientific partnership among the California Institute of Technology, the University of California and the National Aeronautics and Space Administration. The Observatory was made possible by the generous financial support of the W. M. Keck Foundation.

nominal resolving power $\lambda/\Delta\lambda = 47,000$, with the slit projecting to 4.8 pixels on the detector. The bandpass of the three CCD detectors covered 3047–3951Å, 3971–4926Å, and 4977–5894Å, in multiple orders per detector. The slit was set at the parallactic angle, which means that it rotated on the sky during the night. As a result, any atmospheric dispersion was along the slit. We used a slit which was 7×0.86 arcsec on the sky or 4570×562 km at the comet's distance. This slit was much smaller than the coma of the comet so we were imaging only the inner coma. A complete description of the observations, including a log of the time of observations and the angle of the slit on the sky, can be found in Cochran et al. (2006; hereafter Paper 1) [3]. In addition, observations were obtained with the HIRES instrument on 30 May 2005 and 5 and 6 July 2005 UT (the observations of 30 May and 4 July were obtained under Director's time and are available to the public from the Keck archive).

Had their been no impact, we would have observed the ambient gas outflow of the comet. In that case, we would normally extract the spectrum of the comet along the whole 7 arcsec slit. The continuum would be removed by the use of solar analogue stars scaled to the comet's continuum. This would then result in the cometary gas spectrum of the inner coma. However, the impact of the comet and the spacecraft caused additional material to be released from the nucleus and it is this additional material that we wished to monitor.

As a first step, we performed the extraction of the spectrum along the complete length of the slit and attributed any changes in the spectrum with time to the effects of the impact. A complete description of this process, along with sample spectra are included in Paper 1. While this technique is instructive, it is difficult to understand the magnitude of the changes from the impact because the ambient spectrum is so dominant in the earliest times after impact. Therefore, we needed to find a way to remove the ambient spectrum from the spectra recorded on 4 July.

The removal of the ambient spectrum proved difficult because we did not have a representative ambient spectrum prior to impact. We obtained one spectrum of the comet just before the impact on 4 July. However, that spectrum was obtained prior to astronomical twilight; the 720 sec observation was started at 05:36:15 (eight degree twilight was at 05:29UT; 12 degree twilight (nautical) was at 05:58UT; 18 degree twilight (astronomical) was at 06:28). Thus, the sky was still very bright. The sky spectrum is also a solar spectrum of a different color and with a different Doppler shift than the comet's continuum. When we removed the solar continuum from this pre-impact spectrum, we were left with a very noisy spectrum.

We obtained three spectra of the comet on 30 May 2005. These too proved unsuitable to be representative of the ambient comet in July because they were obtained at different heliocentric (1.55 AU vs. 1.51 AU) and geocentric (0.75 AU vs. 0.91 AU) distances than the 4 July data. In addition, the comet was observed to undergo many outbursts between 30 May and 4 July.

To try to minimize the contribution of the ambient coma, we attempted to "isolate" the nucleus within the slit (of course, we did not resolve the nucleus with ground-based observations). To do this, we extracted all of the spectra over the size of the seeing disk, 0.7 arcsec or 457 km. These spectra were generally of much lower S/N than the full slit extractions. These extractions were reported in Paper 1 and example spectra are shown in that work.

While the approach of using a small aperture minimizes the contribution of the outer (ambient) coma to the observations, the impact was an impulse of short duration and the material flowed quickly out of the small seeing disk-based aperture over which we extracted spectra. In this short distance, photodissociation will be unimportant and the spectrum would not show very much change. Thus, our approach of extracting spectra over only a relatively small aperture would not gain the most information from the impact.

Instead of arbitrarily limiting the aperture to the size of the seeing disk, we decided to follow the impact gas as it flowed outwards. After the impact, we expected to see the amount of gas released from the nucleus enhanced over the ambient output. The gas then flowed outwards. When our aperture was filled, the excess emission would again decrease. We used the filling of the aperture to derive a minimum outflow velocity for the CN of 0.51 km sec^{-1} in Paper 1. This value is in agreement with the OH outflow velocity of 0.5 km sec^{-1} determined by Schulz (2006), [14] with XMM Optical observations.

By assuming that material was released at the instant of impact, adopting an outflow velocity of 0.55 km sec^{-1} and assuming that the material flows outwards symmetrically, we can predict the distance the gas would have traveled from the nucleus by the mid-time of each observation. This is shown in Table 1.

Table 1. Post-impact gas outflow

File number	Start time	Mid time	Exposure time (sec)	Elapsed time (sec)	Km† traveled	Pixels† traveled
66	05:55:18	06:08:18	600	496	273	1.7
67	06:06:12	06:11:12	600	1150	633	4.1
68	06:17:05	06:24:35	900	1953	1074	6.9
69	06:32:59	06:40:29	900	2907	1599	10.2
70	06:48:53	06:56:23	900	3861	2124	13.6
71	07:04:47	07:12:17	900	4815	2648	17.0
72	07:20:42	07:28:12	900	5770	3174	20.3
73	07:36:36	07:44:06	900	6724	3698	23.7
74	07:52:29	07:59:59	900	7677	4222	27.1
75	08:08:25	08:15:55	900	8633	4748	30.4
76	08:24:19	08:31:49	900	9587	5273	33.8
77	08:40:13	08:55:13	1800	10991	6045	38.7
78	09:11:10	09:26:10	1800	12848	7066	45.3

† Value at the mid-time

To "follow the gas", we extracted the spectra centered on the optocenter and with an extraction length equal to plus-or-minus the pixel length indicated in the last column of Table 1. The material would reach the full length of the slit (±14.5 pixels) after the fifth observation (file number 70). After this point, denoted with a small gap in Table 1, we were no longer able to continue to follow the impact-derived gas completely. For these subsequent spectra, we extracted data over the complete length of the slit.

For the first four observations, the ends of the slit contained only the ambient cometary spectrum. We extracted spectra covering the first and last 3.5 pixels along the slit for each of the first four spectral files obtained (66–69). Then we averaged these spectra to increase the S/N. We assumed that these averages were representative of the ambient cometary spectrum.

We were concerned that the photodissociation of the species would cause the amount of gas measured at the ends of the slit to be lower than would be true near the nucleus and thus would not be representative of the ambient spectrum on the optocenter. However, not much photodissociation should take place in 2000 km. To check that this was a small effect, we extracted the pre-impact spectrum from 4 July with varying sized apertures corresponding to the values in the last column of Table 1. We verified that, within the noise, the spectra were the same. Thus, we felt justified in using the spectra from the ends of the slit as representative of the ambient spectrum of the comet. These spectra had higher S/N than the pre-impact spectrum, with its bright blue sky.

Once the spectra were extracted, we used observations of a ThAr lamp to assign a dispersion curve to each order. Typical rms errors of the wavelength solution were 0.004 Å. The cometary spectra were then Doppler shifted to the spectrograph rest frame using the orbital information. We next used Mauna Kea Observatory mean extinction coefficients to correct the spectra for signal outside the atmosphere. For the highest airmass observations at the bluest wavelengths (typically below about 3300 Å) at the end of the night, these corrections are not accurate since no flux was received through the atmosphere to correct.

In order to be able to intercompare observations, we needed to normalize the observations to a unit time and pixel. In practice, we normalized to 15 minute observations, since this was the most common exposure time. In addition, we normalized to a unit of 2 pixels (i.e. we divided by the pixel value in the last column of Table 1).

Next, we removed the contribution of the continuum which results from the solar light being reflected off the dust. Finally, we removed the ambient comet spectrum by subtracting the spectral average (normalized similarly to the other spectra) which we derived from the ends of the slit. These ambient spectra were generally devoid of any solar continuum so the solar spectrum did not need to be removed (the dust is the only component which showed a significant change along the length of the slit). At this point, we had a series of spectra which were the gas component that resulted from the impact, per unit time and spatial interval, outside the atmosphere.

2 Behavior of the Gaseous Species

The molecules which are typically observed within our bandpass in spectra for comets at ∼1.5 AU would include OH, NH, CN, C_3, CH, C_2 and NH_2. The emission spectra are generally formed by resonance fluorescence. All of these species are daughters or granddaughters, resulting from photodissociation of their parents. We detected emissions from all of these species. In addition, we observed the O (^1S) atomic line. This line is a prompt emission (it is formed in the excited state) and is generally hidden by the emission of a C_2 band. The C_2 emission from comet Tempel 1 was weak, allowing us to detect the atomic oxygen.

Observations with the instruments on board the Deep Impact spacecraft indicated that, of the 19 GJ impact energy, less than 1 GJ went into a change of the orbit of the comet. In the first 1–2 sec, a hot plume was emitted, carrying about 1 ton of hot material. After that time, an additional 10^4 ton of cold material was emitted. Most of the excess impact energy went into kinetic energy of the hot plume. There was a large increase in H_2O detected by the spacecraft. An even larger amount of CO_2 was detected [1].

It is reasonable to expect that there will be thermal decomposition of some of the parent molecules in this hot plume. Typically, when molecules that are thought to be the parents of the observed cometary emission are subjected to large temperatures they form the same kind of radicals that are observed when these same molecules undergo photodissociation. The effect of this hot plume should be limited to our first time step because the Deep Impact Satellite observations indicated that the plume only lasted for a very short time. We would expect that the effect of the hot plume would manifest itself in the production of species essentially instantaneously on our time scale and in the production of new cometary emissions.

The major molecular component of the volatile ice in a cometary nucleus is H_2O. The photodissociation of H_2O produces OH as a dominant daughter product. The (0,0) band of OH has transitions in the UV, at 3080 Å. With the blue cross disperser, we were reasonably sensitive to OH as long as the airmass was not too high. Using our spectra which have the ambient coma removed, we were able to measure the effect of the impact on the production of OH. Figure 1 shows the OH behavior with time. We see that there is a large rise in the intensity of the OH emission until about 2000 sec after impact and after that the signal decays.

Some of the H_2O will dissociate to atomic oxygen, as will the OH. Oxygen has three observed transitions in the visible part of the spectrum: the "green" line at 5577.339 Å is an O (^1S) transition; the "red doublet" at 6300.304 and 6363.776 Å are O (^1D) transitions. Our bandpass included the O (^1S) but not the red doublet. Unlike the molecular bands which we observe, the oxygen lines are not formed by resonance fluorescence or dissociative recombination [4]. Instead, they are prompt emissions and arise from atoms produced directly into the excited ^1S or ^1D states. These transitions are "forbidden" transitions since the ground state is a ^3P state. The red doublet can be present without the green

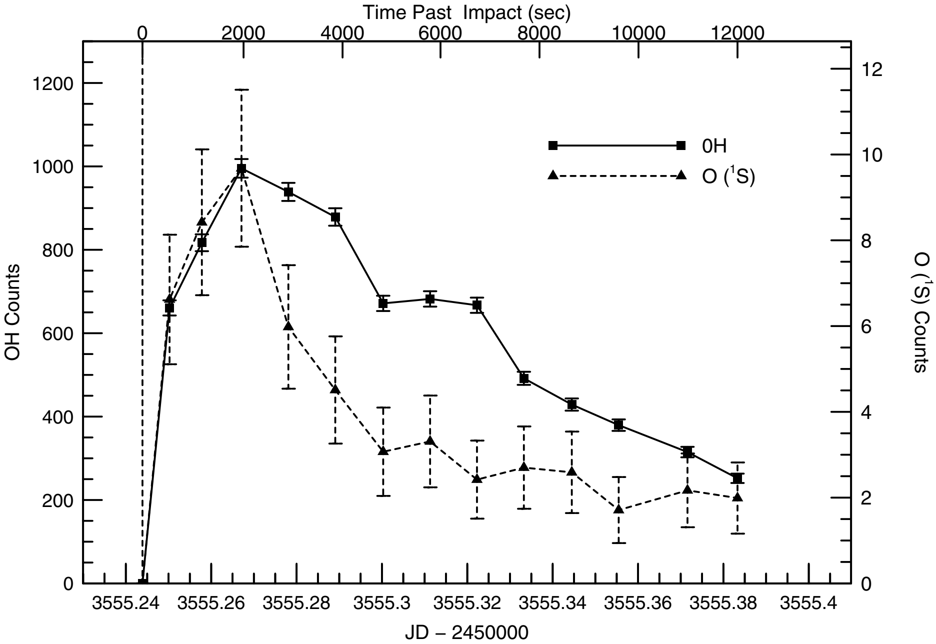

Fig. 1. The integrated flux of 8 lines of the OH (0,0) band are shown along with the deconvolved flux from O (^{1}S). The two species rise together but then the O (^{1}S) decreases more rapidly than does the OH.

line. However, if the green line is present, the red doublet will also be present because 95% of the green line atoms decay via the red doublet (5% decay in the UV). The lifetime of these oxygen lines is believed short, with the ^{1}D lines lasting 150 sec and the green line lasting a mere 1 sec. Thus, if we detect the green ^{1}S line, we are directly tracing the parent. The branching ratios to produce oxygen from H_2O or OH are extremely uncertain. Indeed, it is not clear if the O (^{1}S) line derives from water as that decay product has not been measured in the laboratory. Other potential parents for the O (^{1}S) are CO and CO_2.

Measuring the O(^{1}S) is more complicated than measuring other species. Normally, it is well hidden within the C_2 $\Delta v = -1$ band. Since this C_2 band was weak in comet Tempel 1, we were able to detect the cometary line with little C_2 contamination. However, at the Doppler shift of the comet, the cometary line was partially blended with the telluric O(^{1}S) line. We separated the cometary and telluric oxygen lines by using a 2-Gaussian deconvolution. We show the intensity of the cometary O(^{1}S) in Fig. 1.

By comparing the behavior of the O (^{1}S) with the OH in Fig. 1, we can see that the O (^{1}S) peaked at the same time as the OH but decreased in intensity much more rapidly than did the OH. Since the O (^{1}S) has such a short lifetime and its detection traces its parent, we can conclude that OH is not a major parent for the O (^{1}S). If we plot the O (^{1}S) intensity as a function of $1/\rho^2$, where ρ is the cometocentric distance, we find a linear trend with a slope of 2. This confirms that we are tracing a parent species with the O (^{1}S).

The trend of the OH with cometocentric distance is different than that for O (^{1}S). Once the peak has been reached, the OH decreases as would be expected for the decay of a daughter.

Since the decay of the O (^{1}S) emission follows the parent decay we can conclude that this is a measure of the time dependence of the influx of gas resulting from the impact. It represents the impulse function for the parents that should be present in all of the emissions if all of their parents are produced at the same time and no additional loss mechanism is present. The time dependences of many of the other emissions that we have observed differ from the impulse response of the O atoms. This is as expected since the different species will have different rate constants for formation and destruction.

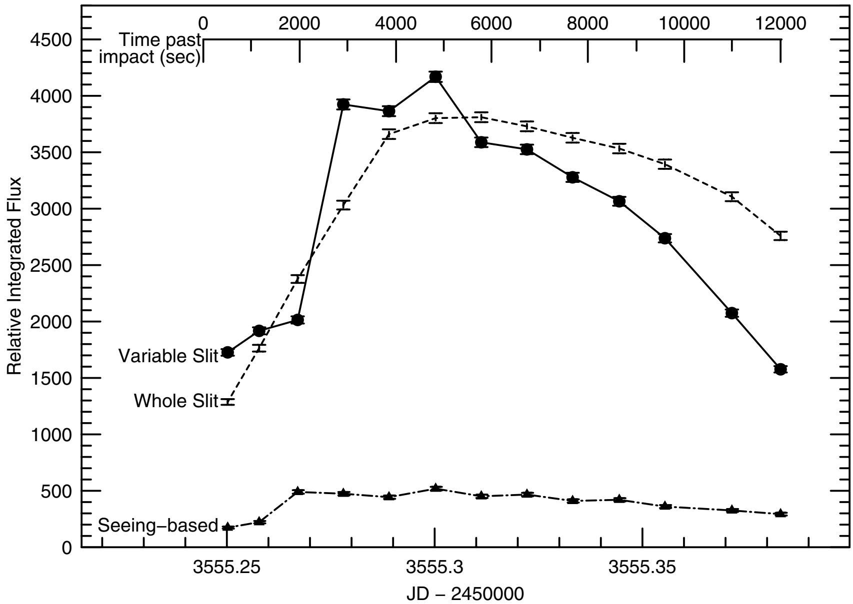

Fig. 2. The integrated line intensities of 19 R and P branch CN lines. The results of this integration for the three different methods of extraction of the spectra (see text) are shown. In the variable slit mode there is an immediate increase in the intensity of the emission followed by a slower rise to a peak intensity at 2907 s. Thus, the intensity in the CN band in the variable slit peaks earlier than the intensity of these bands in the complete slit extraction.

The CN (0,0) band is one of the best studied cometary emission features because it is generally quite strong. The OH (0,0) band is inherently stronger but it occurs at 3080 Å, in the region of strong atmospheric absorption, making it a challenge to detect. The CN band is a $\Sigma - \Sigma$ transition so it has no Q branch. Further, each of the CN rotational lines are unresolved doublets at the comet's outflow velocity and the spectral resolution of HIRES. Each of the unresolved doublet pair rotational lines are well separated from its neighbor, making them easy to measure. The lowest J-level lines of the P branch are to the blue of the bandhead and the P branch wavelengths increase (frequencies decrease) with higher J-levels until about $J = 27$, then the wavelengths decrease, superposing the higher J-level lines on the lower J-level lines. However, lines with $J > 20$ are rarely seen in cometary spectra. The R branch lines have decreasing wavelength with increasing J-level. The (1,1) band overlaps with parts of the R branch but its lines are much weaker than the (0,0) band lines.

We measured the combined intensity of 19 lines of the P and R branch of the (0,0) band of CN by integrating the flux above the local continuum. Figure 2 shows the results of this integration for our three methods of extracting the data. The whole-slit extraction shows the effect of the gas flowing out of the aperture. The rise to the peak is smooth. Our seeing-based (method 2) trend line is the line with the lowest signal/noise. As would be expected, because of the smaller "aperture", the peak emission is earlier than for the whole slit extraction. In addition, the rise to the peak is not as steep from point 1 to 2 as for point 2 to 3. When we use our variable-size aperture to follow the gas outflow, we see a different response of the gas with time. The CN gas does not rise rapidly at the beginning but remains low for the first 2100 s and then rises rapidly. The peak CN emission comes 900 s earlier than it does for the full aperture extraction.

If we look at the trend for individual CN lines we see evidence of the approach to radiative equilibrium. It looks as if the R(1)+ R(0) emission was relatively flat, whereas the R(2) and R(1) increased quickly and peaked early. The $R_1(8)$ + $R_2(7)$ doublet increased more slowly and peaked later. The strength of the higher J-level lines, such as the $R_1(12)$ + $R_2(11)$ doublet, barely changed after the impact.

The OH signal peaked sooner than the CN signal, so either it was flowing outward faster than the CN and reached the edge of our aperture sooner, or it was being formed or destroyed quicker than the CN. The XMM measurement of the OH outflow velocity[14] is consistent with our CN outflow velocity so that the OH radical must have been formed or destroyed sooner than the CN radical. The decay time of the CN radical is actually a factor of 2 shorter than the OH radical [7, 8]. In fact, as Jackson has pointed out, even though the rate constant for the loss of OH radicals can vary with the radial velocity of the comet with respect to the Sun [10], these values are all of the same order or slower than the loss rate for CN. This decay could be due to the decay of the parent rather than the decay of the radical itself because the time response curves can not distinguish between loss of the daughter and loss of the parent. This implies that the parent of CN has to have a photochemical dissociation rate constant that is slower than the corresponding rate constant for water. Fray et al. have recently reviewed the photodissociation rate constants for molecules that are possible parents of CN [5]. When these rate constants are compared to the photodissociation rate constant for the loss of H_2O, all of them but HCN are faster than water. Even HCN decays at about the same rate as water. None of these proposed parent molecules explain the observed differences in the time dependence of OH and CN. It is very unlikely that the parent of OH is anything other than water so the only way that this can be explained is that the emission that comes from OH after the Deep Impact encounter has to have come from the direct production of the radical during the impact event. If ongoing laboratory experiments show that the O (^{1}S) atom is not produced from photodissociation of water then another mechanism will be needed to explain both emissions.

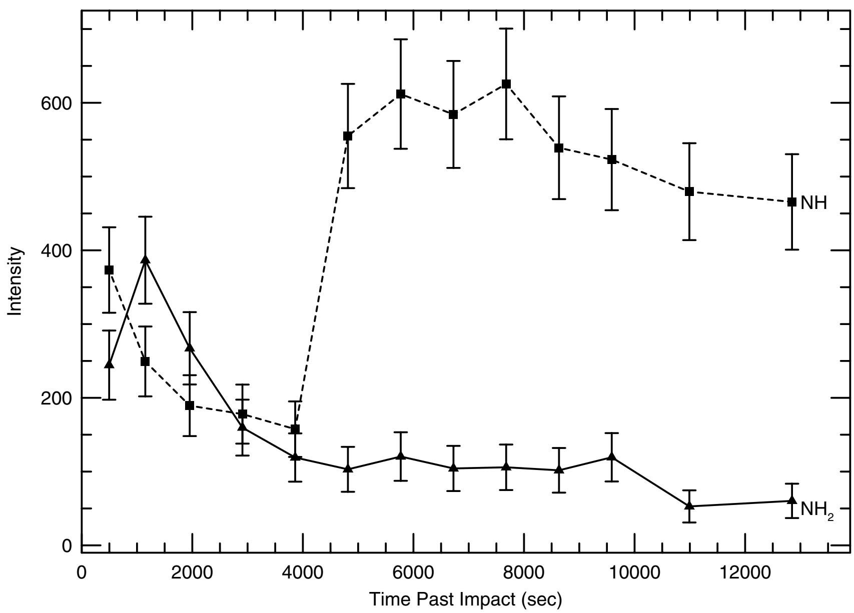

Fig. 3. The integrated flux of the emission from the NH_2 and NH rotational lines. The closed diamonds are for NH_2 and the open squares are for NH emissions. The error bars are the three sigma error bars for a 95 confidence limit. The NH_2 and NH emissions peak more quickly than the OH and O^1S. The NH peaks even quicker than the NH_2.

Figure 3 shows the time dependence on the NH and NH_2 emissions derived from the inner pixels corrected for steady state emission of these emissions in the coma. The NH_2 emission peaks at 1200 s, which is 900 s earlier than both the O (^{1}S) and the OH emission. It is also considerably faster than the CN emission. This implies that the rise of these emissions are not just due to the increase in the concentration of the parents caused by the Deep Impact collision. NH shows a sharp increas around 4000 sec after impact but NH_2 does not increase at later times. It could be that both NH and NH_2 are initially produced in the hot plume but if that is the only way that they were produced then it would not

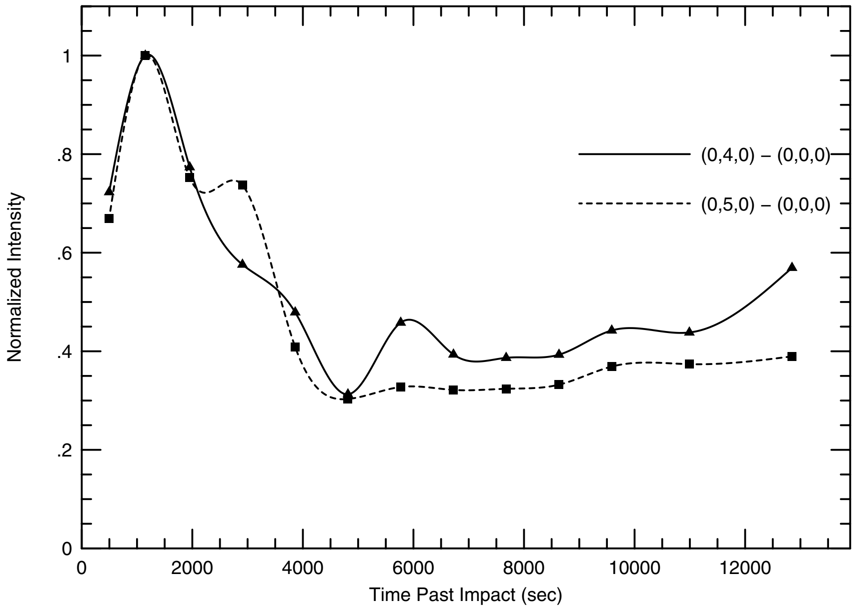

Fig. 4. The integrated flux of the emission from the NH_2 of the $(0,5,0)1_{10}$–$(0,0,0)2_{20}$ and $(0,4,0)1_{10}$–$(0,0,0)2_{20}$ vs time after impact. The trangles are for the (0,4,0) band and the squares are for the (0,5,0) band.

be expected that there would be any increase in the emissions at later times. The NH increase is evidence that an additional amount of NH is produced after the hot plume has been dissipated, even though there is no additional increase in the NH_2. This suggests that the mechanism for the production of the additional NH that peaks later is not due to the commonly assumed mechanism shown in reactions (1) and (2) and implies that NH_3 cannot be the sole parent of both NH and NH_2 since no rise is seen in the NH_2 emission that corresponds to the later rise of NH emission.

$$NH_3 + h\nu_{UV} \rightarrow H(^1S) + NH_2 \quad (1)$$

$$NH_2 + h\nu \rightarrow H(^1S) + NH \quad (2)$$

The random errors for the time dependence of the nitrogen emission are small enough so that time dependence of the curves can be trusted if there are no unknown systematic errors. There is a way of testing for systematic errors by comparing the time behavior of two emission lines that originate from the same lower state. A comparison of such a pair of lines for NH_2 is shown in Fig. 4. The first three points are clearly varying in the same manner, while there are some small differences at later times. Nevertheless the overall trends are almost identical. It also confirms that the overall trends observed in the temporal curves of a species should be a good indication of the true temporal behavior of that species.

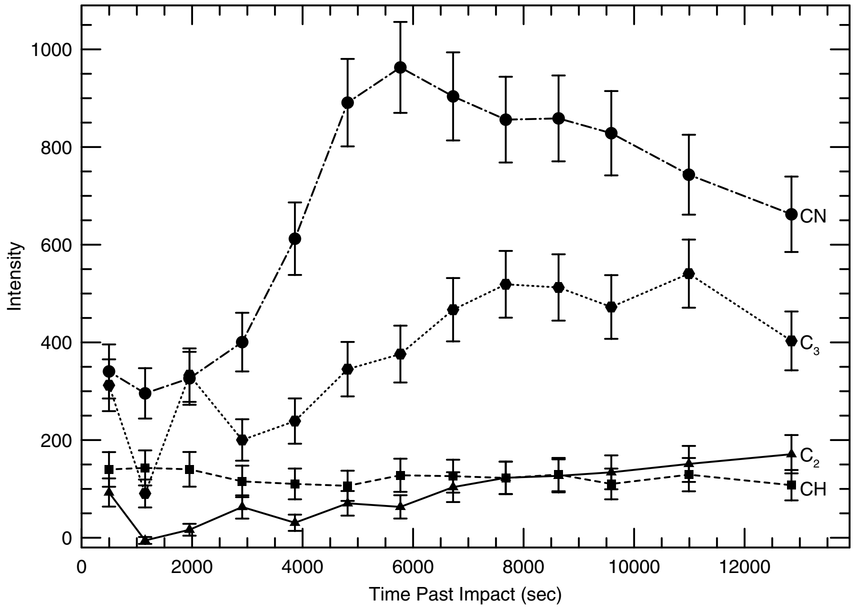

Fig. 5. The integrated flux of the emissions from all of the observed carbon species. C_2 and C_3 show an initial increase and decrease then a steady increase with time, as would be expected for a granddaughter species. CN increases until the aperture is filled and then decreases. CH shows no change of intensity after the impact.

The time dependence of all of the carbon emissions are summarized in Fig. 5. It is clear that there are distinct differences among the different radicals. The CH emission does not change with time, while the others do. However, the CH emission is above the background emission before the event. It may be that this is the signature of a distributed event where the radicals are somehow produced from dust that is emitted as a result of the Deep Impact event.

One of the proposed parents for CH emission is CH_4 via reaction (3).

$$CH_4 + h\nu_{121.6nm} \rightarrow CH + H + H_2 \tag{3}$$

The Keck NIRSPEC team for the Deep Impact collision reported that there was an increase in the CH_4 [13] so the fact that no increase is seen in the CH emission after impact implies that this can not be a significant source of CH in comets. Laboratory studies that involve the direct detection of CH could confirm this observation. The rate constant for the photochemical CH loss is 9.20 x 10^{-3}, which is much faster than the loss rates for OH, CN, and NH_2, so that the rise and fall of this radical should have been even faster than those. It is clear that the CH emission does not change as would be predicted.

C_2 emission is present right after impact and then it decreases and rises at later times. This is consistent with the direct production of C_2 by the hot plume followed by the two step production of the radical from a parent such as acetylene that was excavated as a result of the impact (reactions 4 and 5) [9, 16].

$$C_2H_2 + h\nu \rightarrow C_2H + H \tag{4}$$
$$C_2H + h\nu \rightarrow C_2 + H \tag{5}$$

The temporal behavior of the C_3 emission is similar to the C_2 emission in that it is present right after impact then it decreases, rises again, only to decrease again before rising to a plateau at later times. This is consistent with the proposal that both of these radicals arise as granddaughters rather than daughters. Just as with C_2, the C_3 has an initial rise suggesting that some of it is produced by the hot plume. The material produced at later times is consistent with a two step mechanism involving allene, $H_2C_3H_2$, or propyne, CH_3C_2H via reactions (6) through (9) [11, 12].

$$CH_3C_2H + h\nu_{VUV} \rightarrow HCC_2H + H_2 \tag{6}$$
$$HCC_2H + h\nu \rightarrow C_3 + H_2 \tag{7}$$
$$H_2C_3H_2 + h\nu_{VUV} \rightarrow C_3H_2 + H_2 \tag{8}$$
$$C_3H_2 + h\nu \rightarrow C_3 + H_2 \tag{9}$$

Laboratory studies show that allene produces C_3 more efficiently than propyne which suggests that reactions 8 and 9 may be the most important mechanism for the production of C_3 [15, 6].

To date we have no evidence for the presence of new emissions in the analyzed cometary spectra.

3 Conclusions

The Keck HIRES spectra have been processed to extract the temporal behavior of the CN, NH, NH_2, O (^{1}S), OH, C_2, CH, and C_3 that results from the Deep Impact encounter with Comet 9P/Tempel. The OH and O (^{1}S) have the same initial rise but the later decays faster than the former. The faster decay of the O (^{1}S) confirms that a pulse of gas passes through the coma. The slower decrease of the OH has to be connected with the formation and decay processes that form this radical. The overall temporal behavior of the observed species certainly show that these curves have embedded in them information about how the radicals are being formed. It appears that the hot plume produced in the initial impact initially forms some of the radicals. After the hot plume has passed through the coma the radicals are formed by different mechanisms. In some cases the photochemical processes normally present in comets form some of these radicals during this period. In others there are new mechanisms, yet to be discovered, that are responsible for the observed time dependences. To firmly establish the chemistry requires a detailed evaluation of the range of rate constants that are needed to fit each curve. This is the next stage in the evaluation of the Keck HIRES data.

Acknowledgements We thank Dr. Fred Chaffee for making Director's Discretionary time available pre-impact. Our thanks to Dr. Hien Tran for obtaining the observations of 30 May and 4 July and for help on 5 and 6 July. This work was funded by NASA Grant NNG04G162G (ALC), NASA Grant NNG06A67G (WMJ) and NSF Grant CHE-0503765 (WMJ).

References

1. M. F. A'Hearn. Comets after Deep Impact. Presentation at *Deep Impact as a World Observatory Event – Synergies in Space, Time*, H. U. Käufl and C. Sterken, editors, Springer-Verlag, 2006.
2. M. F. A'Hearn, M. J. S. Belton, W. A. Delamere, J. Kissel, K. P. Klaasen, L. A. McFadden, K. J. Meech, H. J. Melosh, P. H. Schultz, J. M. Sunshine, P. C. Thomas, J. Veverka, D. K. Yeomans, M. W. Baca, I. Busko, C. J. Crockett, S. M. Collins, M. Desnoyer, C. A. Eberhardy, C. M. Ernst, T. L. Farnham, L. Feaga, O. Groussin, D. Hampton, S. I. Ipatov, J.-Y. Li, D. Lindler, C. M. Lisse, N. Mastrodemos, W. M. Owen, J. E. Richardson, D. D. Wellnitz, and R. L. White. Deep Impact: Excavating Comet Tempel 1. *Science*, 310:258, 2005.
3. A. L. Cochran, W. M. Jackson, K. J. Meech, and M. Glaz. Observations of comet 9P/Tempel 1 with the Keck 1 HIRES instrument during Deep Impact. *Icarus*, page In press, 2006.
4. M. C. Festou and P. D Feldman. The forbidden oxygen lines in comets. *Astr. and Ap.*, 103:154, 1981.
5. N. Fray, Y. Bénilan, H. Cottin, M.-C. Gazeau, and J. Crovisier. The origin of the CN radical in comets: A review from observations and models. *Plan. Space Sci*, 53:1243, 2005.
6. J. D. Huang, Y. T. Chen, A. H. Kung, W. M. Jackson, and C.-K. Ni. Photodissociation of propyne and allene at 193 nm with vacuum ultraviolet detection of the products. *J. Chem. Phys.*, 110:3320, 1999.
7. W. F. Huebner and C. W. Carpenter. Solar photo rate coefficients. Informal Report LA-8085-MS, Los Alamos Scientific Lab., Los Alamos, NM, October 1979.
8. W. F. Huebner, J. J. Keady, and S. P. Lyon. Solar photo rates for planetary atmospheres and atmospheric pollutants. *Astrophys. Space Sci.*, 195:1, 1992.
9. W. M. Jackson. The photochemical formation of cometary radicals. *J. Photochem.*, 5:107, 1976.
10. W. M. Jackson. The lifetime of the OH radical in comets at 1 AU. *Icarus*, 41:147, 1980.
11. W. M. Jackson, D. S. Anex, R. E. Continetti, B. A. Balko, and Y. T. Lee. Molecular beam studies of the photolysis of allene and the secondary photodissociation of the C_3H_x fragments. *J. Chem. Phys.*, 95:7327, 1991.

12. W. M. Jackson, Y. Bao, R. S. Urdahl, X. Song, J. Gosin, and C. Lu. Cometary implications of recent laboratory experiments on the photochemistry of the C_2H and C_3H_2 radicals. In A. W. Harris and E. Bowell, editors, *Proceedings of the International Conference held at Northern Arizona University, Flagstaff, USA, Asteroids, Comets, Meteors 1991*, page 253, Houston, 1992. Lunar and Planetary Institute.
13. M. J. Mumma, M. A. DiSanti, K. Magee-Sauer, B. P. Bonev, G. L. Villanueva, H. Kawakita, N. Dello Russo, E. L. Gibb, G. A. Blake, J. E. Lyke, R. D. Campbell, J. Aycock, A. Conrad, and G. M. Hill. Parent volatiles in comet 9P/Tempel 1: Before and after impact. *Science*, 310:270, 2005.
14. R. Schulz. Detection of icy grains with XMM optical monitor. Presentation at *Deep Impact as a World Observatory Event – Synergies in Space, Time*, H. U. Käufl and C. Sterken, editors, Springer-Verlag, 2006.
15. X. Song, Y. Bao, R. S. Urdahl, J. N. Gosine, and W. M. Jackson. Laser-induced fluorescence studies of C_3a formation and isomerization in the 193 nm photolysis of allene and propyne. *Chem. Phys. Lett.*, 217:216, 1994.
16. O. Sorkhabi, V. M. Blunt, H. Lin, M. F. A'Hearn, H. A. Waver, C. Arpigny, and W. M. Jackson. Using photochemistry to explain the formation and observations of C_2 in comets. *Plan. Space Sci.*, 45:721, 1997.

Springer
http://www.springer.com/978-3-540-76958-3

Deep Impact as a World Observatory Event: Synergies in Space, Time, and Wavelength
Proceedings of the ESO/VUB Conference held in Brussels, Belgium, 7-10 August 2006
Käufl, H.U.; Sterken, C. (Eds.)
2009, XX, 331 p., Hardcover
ISBN: 978-3-540-76958-3